

## Lab-scale Investigation of a Multi Well Enhanced Geothermal Reservoir

Lianbo Hu, Ahmad Ghassemi

Reservoir Geomechanics and Seismicity Research Group

The University of Oklahoma, Norman, OK 73019 USA

ahmad.ghassemi@ou.edu

**Keywords:** Enhanced geothermal systems, hydraulic fracture, acoustic emission, tracer, thermal drawdown

### ABSTRACT

The performance of the Enhanced or engineered geothermal system (EGS) is highly dependent on the fracture system thus a good understanding of the fracture properties is essential for estimating /evaluating the performance of the system. In this work, we study the fluid/heat flow properties of the hydraulically induced fracture properties on a laboratory scale using cold water circulation and tracer analysis. To achieve this goal, we first performed reservoir stimulation on 13x13x13 inch<sup>3</sup> cubical rock samples under representative in-situ stress regimes to establish a hydraulic connection between the central injection well and production wells drilled nearby. And then the rock block was heated to a uniform temperature of 70 degrees Celsius. Zero-degree cold water was injected into the central well and heated water collected from the production wells. Tracer test was conducted to investigate the fracture volume and connectivity between injection and production wells. During circulation, temperature in the wells and on the block surfaces was recorded. The maximum temperature drop was as high as 52.6 °C in the injection well and about 23.8 °C in one production well and 10 °C in another production well. Heat extraction analysis shows that about 12% of the geothermal energy stored in the heated rock was extracted during circulation. Tracer test was conducted after circulation phase, the result from the Method of Moment indicates the fracture volume is 3.66ml. 3D fracture geometry was reconstructed after the tested block was cut into slabs. And the fracture area calculated from the 3D fracture geometry is 224.5 cm<sup>2</sup>, which yields that the fracture aperture is 163um. The fracture geometry and production capacity is good agreement with numerical simulations. .

### 1. INTRODUCTION

Addressing questions related to reservoir creation in different rock types and stress conditions, and good characterization of the induced or activated fracture system is necessary for removing barriers for large scale EGS utilization. Laboratory scale studies present a good opportunity to help resolve some of the pending challenges since Lab-scale simulation can be conducted with well-controlled boundary conditions and provide better access to the fracture. The main purpose of this project is to gain a better understanding of the geometry and the heat exchange properties of the hydraulically induced fractures in EGS. To realize this goal, we have carried out a number of hydraulic fracturing and circulation experiments using 13x13x13 inch<sup>3</sup> cubical granite rock samples under representative in-situ stress regimes. The design consists of a central injector and 4 producers in a five-spot arrangement. The injector is hydraulically fractured to connect with the producers. The system is then heated to a desired temperature and circulation as well as tracer tests are carried out to characterize the fracture. The following sections describe the results of a recent test.

### 2. THE LAB-SCALE EGS TEST SYSTEM

Figure 1 (right) shows the fully assembled EGS test systems. The system has several integrated subsystems to recreate a small-scale geothermal reservoir and to simulate the geothermal development by water circulation. The main subsystems are: a polyaxial frame and heaters, hydraulic fracturing and circulation systems, temperature, data acquisition systems, and fluids and tracers. Figure 1 (left) is a picture of the polyaxial loading frame which can be sealed with high pore pressure inside and heated up to 90 °C by water circulation. More information about these subsystems is provided by Hu et al., 2016. Sensors on the block surfaces and within surface cavities and wellbores are used locate acoustic emissions caused by the stimulation and to monitor local changes in fluid pressure, and temperature. The polyaxial frame can be sealed with high pore pressure in the test block and may be pre-heated to simulate a geothermal system. Multiple wells can be drilled into the test block to simulate injection and production. Fluid produced from the production wells is collected and analyzed.

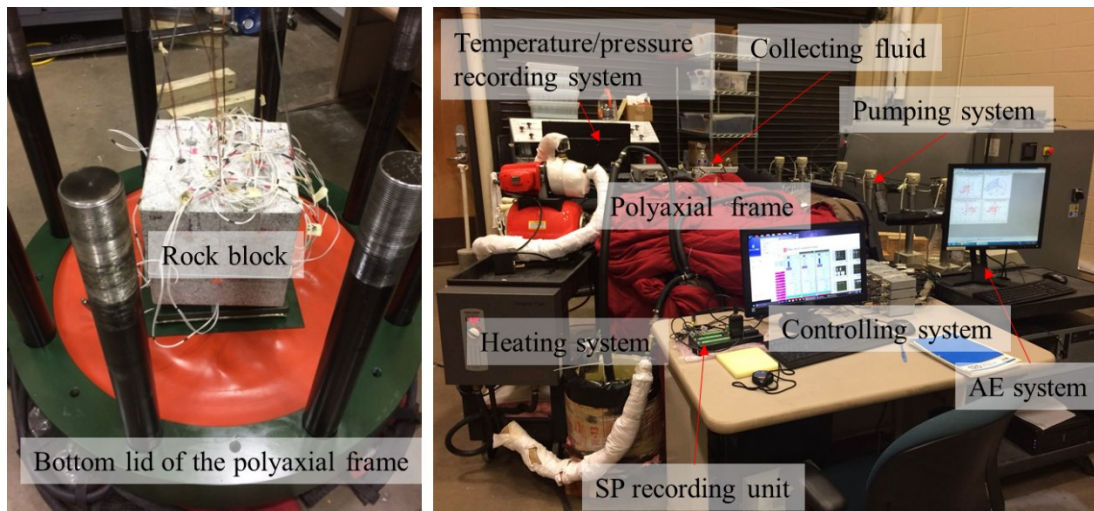


Figure 1: Partially assembled polyaxial loading frame (left) and the fully assembled EGS test system (right).

### 3. LABORATORY TEST RESULTS

#### 3.1 Test Setup

Figure 2 (left) is a top view showing the layout of the wells and sensors on the top surface of the Sierra White granite block, and Figure 2 (right) is a longitudinal sectional view of the sample showing the interior layout of the wells. The injection hole was drilled with a 0.75 inch diameter drill bit. The injection well has a drilled depth of 7.5 inch and a diameter of 0.79 inch. A circular notch was created at the injection wellbore at the depth of 6.5 inch. High strength epoxy was poured into the hole to seal the annulus between the injection tubing and the wellbore wall, leaving a 2.0 inch unsealed injection interval at the bottom. Four production wells with depths of 9.0 inch were drilled 3.5 inches away from the injection well and have 5.0 inch unsealed production intervals at the bottom. The diameter of the production wells is 0.51 inch. A thermistor was located at the center of each downhole unsealed interval to measure temperature histories. Epoxy cylinders with slightly smaller diameters than the wellbore were used to minimize the open space in the wellbores thus minimizing the effect of wellbore storage. The space between the rock block and the inner surface of the loading frame is occupied by flatjacks, PEEK plates and steel plate spacers. After the sample was put into the frame and the frame was fully assembled, principal stresses were applied by injecting oil into the flatjacks to predetermined pressure levels. To contain the induced fracture within the rock block, the hydraulic fracturing process was conducted carefully with real-time AE and pressure monitoring using a LABVIEW program.

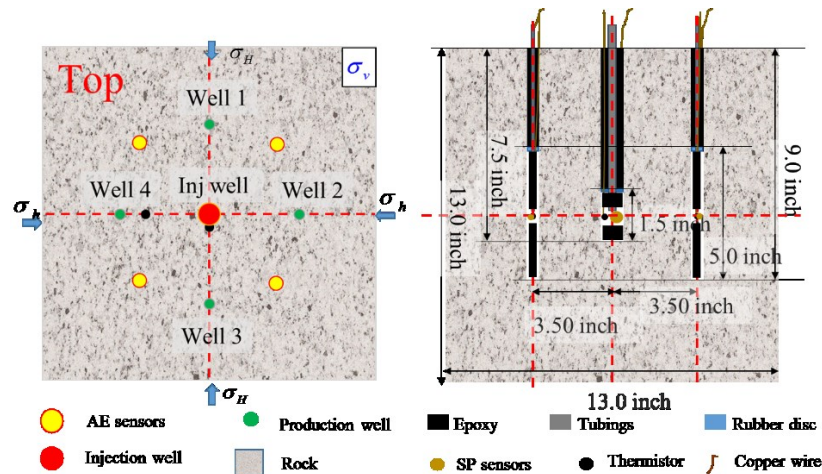


Figure 2: Layout of injection well (left) and production wells with sensors (right)

#### 3.2 Hydraulically Induced Fracture

At first, hydraulic fracturing test was conducted without fluid in the frame and the stress conditions listed in Table 1. The stress state was arranged to allow a horizontal fracture to form in the block. The test was conducted on a block whose inner parts around the production and injection wells were saturated. The saturation was performed by maintaining the pressure at a level of 250 psi in the injection well and 100 psi at the production wells for 62 hours. In total, 144.8 ml 0.002 mole/L NaCl was injection in to the rock before fracturing test. The injection fluid was also 0.002 mole/L NaCl solution. For better control of the fracture propagation, the injection rate was set to be 1.0 ml/min. The hydraulic fracturing test was conducted at room temperature. And when the injection pressure drop exceeded the preset value, the pump ceased. Also, if the pressure in a production well experienced a rapid increase (about 10 psi per second), the valve for that well was opened to avoid fracture reaching the rock surfaces. In this way we were able to steer the fracture to contain with the rock block.

**Table 1: Experimental parameters for Sierra White granite block**

$\sigma_V$ , psi	$\sigma_h$ , psi	$\sigma_H$ , psi
500	1000	1500

After the fracturing, heating and circulation stages of the test, the block was cut into slabs and then fluorescent penetrant was applied on the cutting surface. Figure 3 shows the slab cutting through the injection with detail information at the notch. From this picture, it is clear that the induced fracture intersects Well No.4 and it is only a few millimeters away from Well No.2. Based on the fracture traces on all the slabs, the fracture geometry was reconstructed in 3D and is shown in Figure 4. The reconstructed fracture shows that the induced fracture intersects Well No.3 and Well No.4 and it is very close to Well No.2. From Figures 3 and 4, the induced fracture is quite flat and does not reach the rock block surfaces. The fracture does not propagate equally in all direction and this likely is the result of the rock heterogeneity and the fact that the viscosity of the fluid is very low so the fracture tends to follow the weak grain boundaries. The fracture geometry indicates that hydraulic connectivity between the injection well and production wells are different. The differences are in fact reflected in production, circulation, and tracer data.

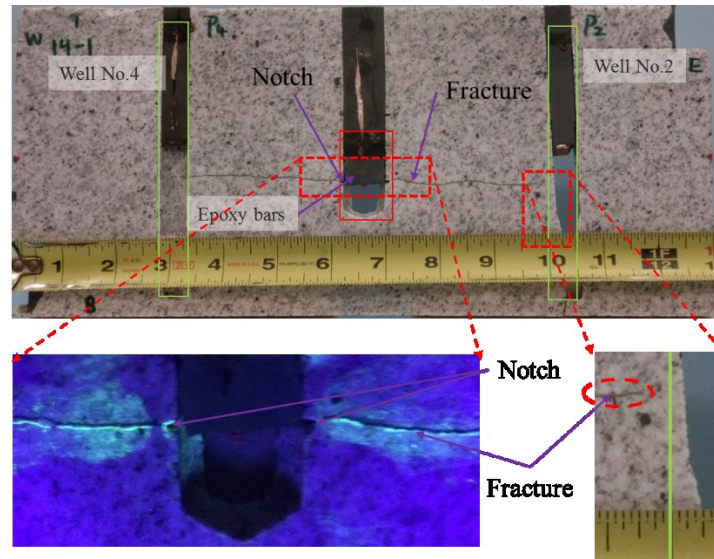


**Figure 3: Pictures of the slab cutting through the injection with detail information at the notch**

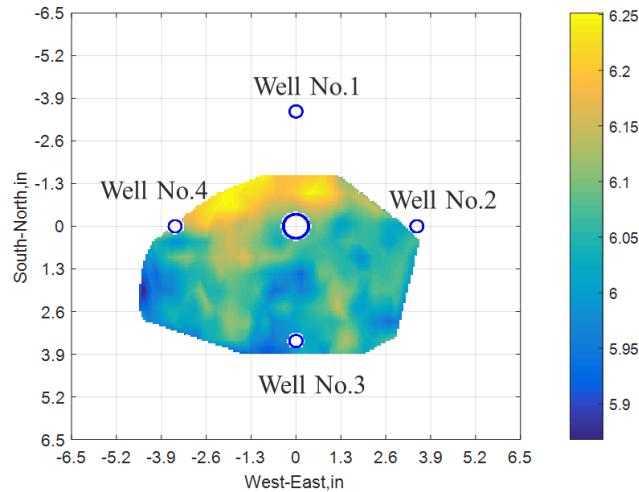


**Figure 4: 3D reconstructed fracture geometry**

The fracture surface profile was quantified with a laser scanner. Based on the digitized profile, the first-derivative root-mean-square,  $Z_2$ , was used as a parameter to obtain the joint roughness coefficient (JRC) of the fracture (Tse and Cruden 1979, Yu and Vassade 1991). The

hydraulic tortuosity of the fracture which is the ratio of the length of the fracture to the distance between its ends was also calculated and compared with a tensile fracture from the Brazilian test. Figure 5 (top) is a surface profile of the Brazilian test fracture and Figure 5 (bottom) is for the hydraulically induced fracture. The JRC value and tortuosity for the hydraulically induced fracture are 12.1 and 1.022 respectively. These two parameters for the Brazilian fracture surface are 9.7 and 1.017 respectively.

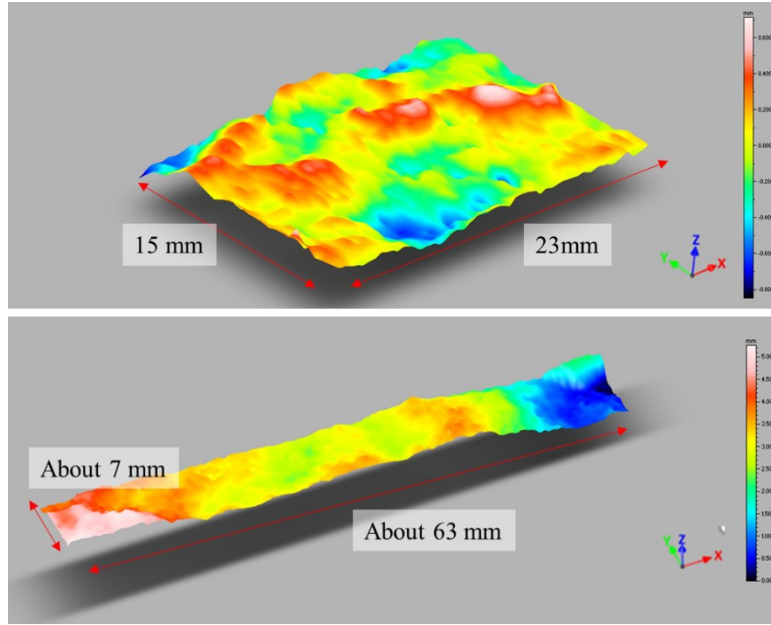


**Figure 5: Surface profile of the Brazilian test fracture (top) and the hydraulically induced fracture (bottom)**

**3.4 Circulation Test Results**

After the fracturing stage was completed, 0.002 mole/L NaCl solution was poured into the frame and then the heating system was connected to heat the whole polyaxial frame. After about 18 hours of heating, the granite block was heated to a near uniform temperature of 69°C. Then, cold 0.002 mole/L NaCl solution was injected into the injection well. By putting cold packs around the injection pumps and pre-cooling the injection fluid and also placing a long section of the injection tubing into an ice water tank, the temperature of the injection fluid before entering the polyaxial frame was maintained near zero Celsius. To prevent the further fracture propagation during circulation, the injection rate was increased step by step while monitoring AE. During the whole period of the circulation test, the pressure at the production wells was close to the atmosphere pressure by opening the valves controlling the production. At the beginning, the injection pressure increased to a peak value about 3000 psi with an injection rate of 2 ml/min. The high pressure and the subsequent pressure drop indicate possible partial healing of the hydraulic fracture during the heating process. Subsequently, the pressure continued to decrease even while increasing the injection rate. This can be attributed to the cooling effect of the matrix around the fracture. As a result of using higher injection rates, the temperature of the injection well and the rock was lower more causing a larger fracture aperture and thus a higher permeability. At the end of the circulation phase, the injection rate was 25 ml/min and the injection pressure was maintained at about 920 psi.

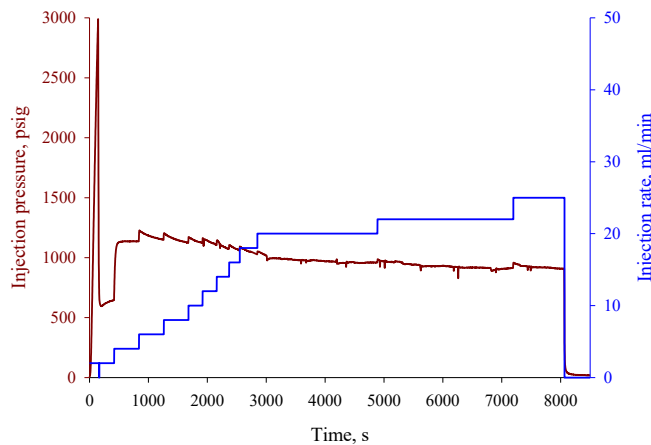


**Figure 5: Injection flowrate and pressure during circulation test**

The water produced from the production wells was collected and the production rate was calculated based on the produced fluid weight and collection time for each sample. The water recovery percentage was calculated as the ratio of the produced water to the injected water. Figure 7 shows the injection rate, production rate and water recovery percentage. With injection rate of 25 ml/min, more than 97.5% of

injection fluid was recovered from production wells. Well No.3 and No.4 produced 82.8% and 14.8% of the injected fluid in the last stage, respectively. And the total flow in other two production wells was less than 1.0% of the injection rate due to lack of direct fracture connection with the injector. The flow rate in Wells No.1 and No.2 were negligible. Since the fracture had crossed Well No.3, the flow rate was much higher than Well No.4. The flow advantage into Well No.3 seems to have enhanced with time since the temperature of the fracture connecting the injection well and Well No.3 is lower due to the high fluid rate flowing into the fracture. The water recovery percentage indicates that higher injection rate results in a higher recovery rate, however, this can also lead to short-circuiting, suggesting the need for flow management in multi-frac EGS and the desirability of a complex fracture network.

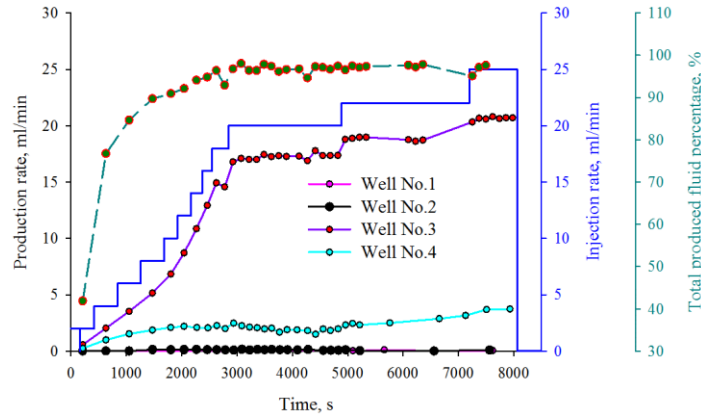


**Figure 7: Flow rate in wells and water recovery percentage**

Figure 8 shows the temperature in the wells and the injection rate information during the circulation test. The temperature at the bottom of the injection well decreased with continued injection and at higher injection rates, while the temperature change in the production wells was very small before  $t=1400s$  (there are two reasons for this: when the injection rate was low, the injected water was heated up to the block temperature before it reached the bottom of the injection well, and the cooling front had not reached the production wells yet). After a long time of circulation, the well temperatures were: injection well: 16.9°C; Well No.1: 64.6°C; Well No.2: 64.2°C; Well No.3: 45.3°C; Well No.4: 59.0°C. The temperature drops in these wells are 52.6°C, 4.5°C, 4.8°C, 23.8°C and 10.0°C, respectively. It is quite clear that since most of the injected water flows to Well No.3, it has the highest temperature drop among the production wells. The temperature decreases in Well No.1 and No.4 results from the cooling of the central part of the granite block due to production.

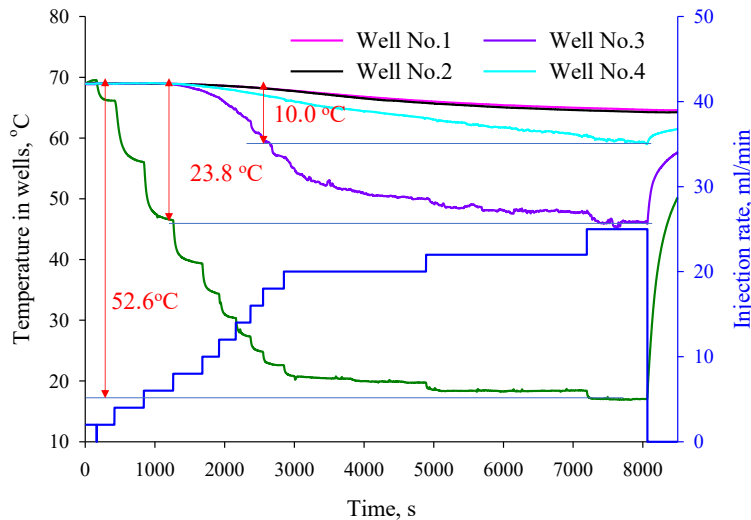


**Figure 8: Temperature in wells**

Figure 9 shows the temperature variation on the rock block surfaces. During the circulation test, the temperature variation on the North, East and Bottom surfaces was less than 1 °C. The temperature change on the top surface near the injection tubing has the maximum variation (14.5°C). The temperature drop on the top surface and 2.5 inch away from the injection tubing was about 2 °C. The influence of the injection tubing is limited to a couple of inches around the tubing based on the temperature change of the two points on the top surface.



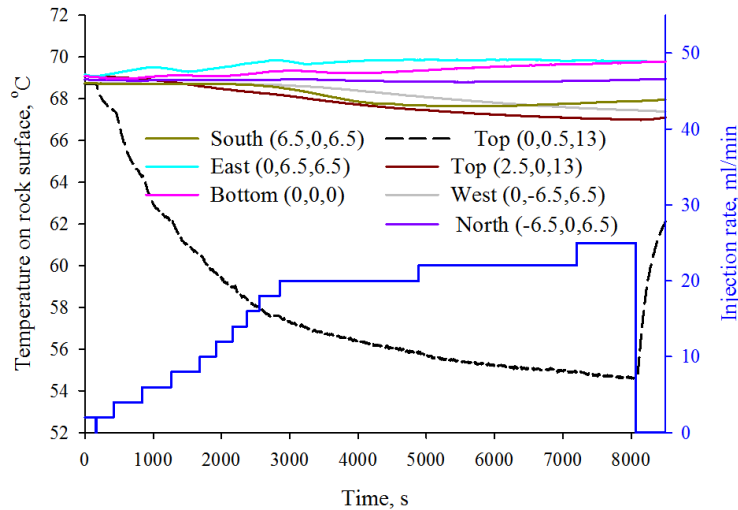


**Figure 9: Temperature on rock surfaces**

Although it is difficult to determine the fracture fluid/heat flow properties analytically, it is very useful to estimate how much heat was extracted during the circulation test. At first, the water temperature at the injection wellhead was estimated based on its temperature at the water tank and at the bottom of the injection well. With estimated water temperature at the wellhead of the production well, the temperature increase was calculated. Note that the injected water is heated not only when it flows through the fracture but also when it flows in the wellbore. And due to lab-scale of the block, the extracted heat through the wellbore cannot be neglected, and thus the extracted heat by flow through both fracture and wellbore were calculated, Figure 10 shows the calculation result. Only the flow in Well No.3 and Well No.4 is considered because the flow rate in other two wells is much smaller. Based on the flowrate and the production temperature, the extracted heat was calculated by integrating the heat extraction rate curve from the beginning to the end of the circulation. Figure 10 shows that a higher injection rate results in a higher heat extraction rate, and about 74% of the extracted heat is from the water flowing through the fracture. The heat extraction rate through fracture is estimated to be 53J/s. The geothermal energy stored in the heated rock before circulation is calculated using room temperature as a reference. The total heat extracted during the circulation phase is estimated as 12% of the heat energy stored in the rock block.

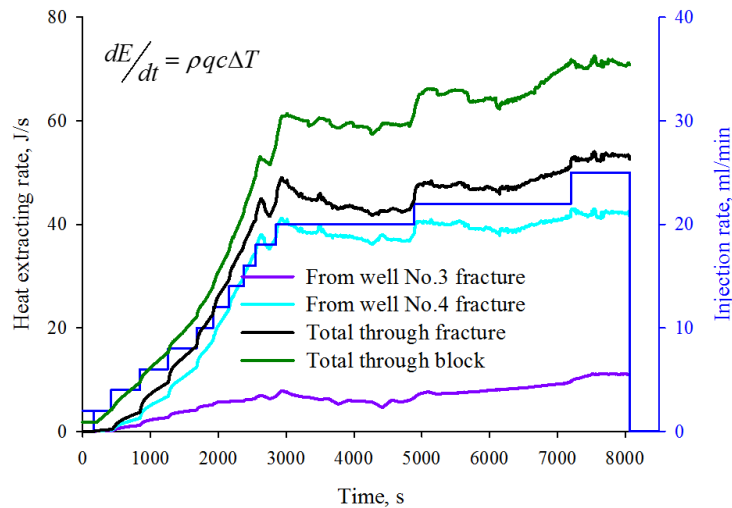


**Figure 10: Heat extraction rate from the test granite block**

#### 4. Tracer Test Result

After the circulation test, a tracer test was carried out. The tracer test had three phases according to the concentration of the injection fluid as shown in Figure 11. During Phase #2 the injected solution was 1 mole/L NaCl (PPM: 58440, around 500 times higher than pore fluid) and in Phase #1 and Phase #3 the injected solution was 0.002 mole/L NaCl. The injection rate was 1 ml/min. The Method of Moment is applied to analyze the tracer test result. The Method of Moment assumes a steady state flow for the tracer fluid. So a normal concentration fluid was injected to establish the steady flow before tracer was injected. It is also useful to have some fluid sample produced before tracer injection to get the background fluid concentration in the fracture. Since the production rate was very low and the injected volume of the high concentration fluid was small, the collected fluid from the wells was diluted and then the conductivity was measured. The concentration of the produced fluid was calculated based on the conductivity of the resulting fluid. Figure 12 shows the concentration of the injection and production fluid. In Well No.3 and Well No.4, we observed the two apparent linear relationships of the trace tail on the

semi-logarithmic plot shown in Figure 12. The first one was dominated by the fracture volume, pipe volume and the unoccupied volume in the open interval of the well, while the second open interval is due to the rock matrix leak-off. Numerical simulations of the tracer concentration evolution during injecting a pulse of partitioning tracer into a shale gas reservoir (e.g., Tian et al, 2016) also shows this phenomenon. Because the test was stopped, the second linear tracer tail in is not observed in the other wells. Based on the method of moments and the first linear relationship of the tracer tail, the estimated fracture volume is 3.66 ml. The estimated fracture area from the reconstructed 3D fracture geometry is 224.5 cm<sup>2</sup> from which we calculate the average fracture aperture to be about 163µm. It is very difficult to get the real tracer swept volume accurately, since the fracture volume in lab-scale is very small and also the tracer recovery percentage is small. However, it can still reveal the connectivity quality between the injection and production wells (by peak value and the peak arrival time).

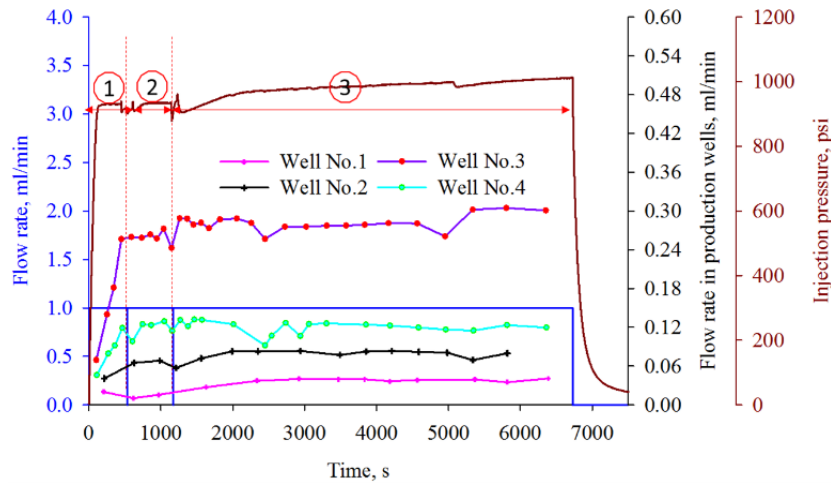


Figure 10: Flow rate of the injected and produced fluid and the injection pressure

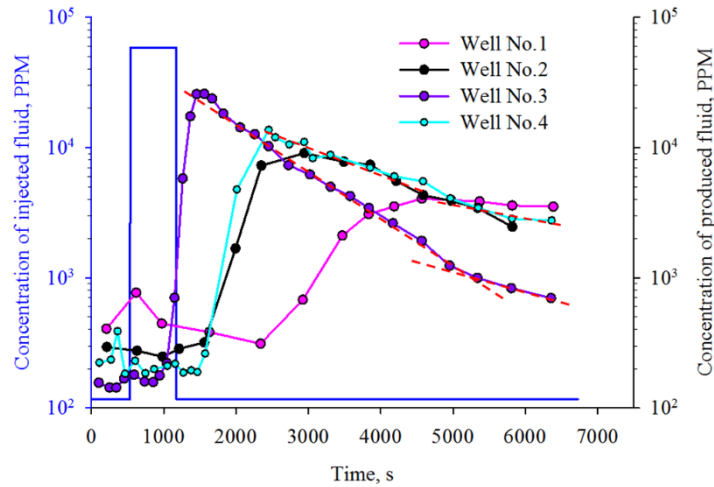


Figure 11: Concentration of the injected and produced fluid

The injection pressure is also plotted in Figure 10. It can be seen there was no major pressure drop during the test, which indicates no new fracture were generated during the tracer test, so the tracer result can be applied to analyze the geometry of the original fracture in the block.

## 5. CONCLUSION

We have performed reservoir stimulation using 13x13x13 inch<sup>3</sup> cubical Sierra White granite samples under representative in-situ stress regimes to create a fracture create and to establish the hydraulic connection with the central injection well and production wells. And then the rock block was heated up to a uniform temperature about 70 °C. Cold water was injected into the central well and collected from nearby multi production wells to simulate the geothermal development in Lab-scale. Tracer test was conducted to investigate the fracture volume and connectivity between the injection well and production wells. During circulation, temperature in the wells and on the block surfaces was recorded. The maximum temperature drop was as high as 52.6 °C in the injection well and about 23.8 °C in one production well and 10 °C in another production well with injection rate of 25 ml/min. Since the induced fracture does no reach the rock surface and the rock matrix permeability is relatively low, the water recovery percentage is about 97.5%. Tracer test data show some results predicted

by numerical simulations, and the fracture volume was calculated with method of moments. 3D fracture geometry was reconstructed after the tested block was cut into slabs. The fracture volume obtained from tracer analysis is 3.66 ml, which yields an average fracture aperture of 163µm based on the reconstructed 3D fracture geometry. Modeling of the performance of the Cooper Basin EGS system by Grant and Garg (2012) indicated a recovery factor of less than 2%. This is much lower than the conventional values of up to 70% that have been used in generic studies. Our lab results show a recovery of 12% during circulation.

#### ACKNOWLEDGEMENTS

This project was supported by the U.S. Department of Energy Office of Energy Efficiency and Renewable Energy under Cooperative Agreement DE-EE0006765.0000. This support does not constitute an endorsement by the U.S. Department of Energy of the views expressed in this publication.

#### REFERENCES

- Tse, R. and Cruden, D.M., 1979, October. Estimating joint roughness coefficients. In International journal of rock mechanics and mining sciences & geomechanics abstracts. Vol. 16, No. 5, pp. 303-307
- Yu, X. and Vayssade, B., 1991, July. Joint profiles and their roughness parameters. In International journal of rock mechanics and mining sciences & geomechanics abstracts. Vol. 28, No. 4, pp. 333-336
- Wu X, Pope GA, Shook GM, Srinivasan S. A method of analyzing tracer data to calculate swept pore volume and thermal breakthrough in fractured geothermal reservoirs under two-phase flow conditions. In Proceedings, 30th Workshop on Geothermal Reservoir Engineering, Stanford University, Stanford, CA, USA 2002 Jan 31.
- Shook, G.M. and Forsmann, J.H., 2005. Tracer interpretation using temporal moments on a spreadsheet (No. INL/EXT-05-00400). Idaho National Laboratory (INL).
- MIT-Led Report. 2006. The Future of Geothermal Energy, ISBN: 0-615-13438-6.
- Ishibashi T, Watanabe N, Hirano N, et al. 2012. Experimental and Numerical Evaluation of Channeling Flow in Fractured Type of Geothermal Reservoir. *Thirty-Seventh Workshop on Geothermal Reservoir Engineering*, Stanford University, Stanford, California.
- Grant, M.A. and Garg, S.K., 2012, January. Recovery factor for EGS. In Proceedings, 37th Workshop on Geothermal Reservoir Engineering, Stanford University, Stanford, California, USA, January 30 - February 1, 2012
- Tian, W., et al., 2016. Estimation of hydraulic fracture volume utilizing partitioning chemical tracer in shale gas formation, Journal of Natural Gas Science and Engineering, <http://dx.doi.org/10.1016/j.jngse.2016.06.018>
- Hu L, Ghassemi A, et al. 2016. Laboratory Scale Investigation of Enhanced Geothermal Reservoir Stimulation. In Proceedings, 41<sup>st</sup> Workshop on Geothermal Reservoir Engineering, Stanford University, Stanford, California, USA, February 22-24, 2016
- Hu, L., Ghassemi, A., Pritchett, J. and Garg, S., 2016. Laboratory Scale Investigation of Enhanced Geothermal Reservoir Stimulation. 50th US Rock Mechanics/Geomechanics Symposium. American Rock Mechanics Association.
- Hu, L., Ghassemi, A., Pritchett, J. and Garg, S. 2017. Experimental Investigation of Hydraulically Induced Fracture Properties in Enhanced Geothermal Reservoir Stimulation. Proc. 42nd Stanford Geothermal Workshop held in Stanford University, Stanford, California, USA
- Hu, L., Ghassemi, A., Pritchett, J. and Garg, S. 2017. Characterization of Hydraulically Induced Fracture in Lab-scale Enhanced Geothermal Reservoir. In Proceedings, 41st GRC Annual Meeting held in Salt Lake City, Utah, USA